Supplementary information

Switching of the Mechanism of Charge Transport Induced by Phase Transitions in Tunnel Junctions with Large Biomolecular Cages

Nipun Kumar Gupta[†1,2], *Rupali Reddy Pasula*[†3], *Senthil Kumar Karuppannan*[†1], *Zhang Ziyu*[1], *Anton Tadich*[5], *Bruce Cowie*[5], *Dongchen Qi*[6], *Peter Bencok,*[7] *Sierin Lim*[*3,8], *Christian A. Nijhuis*[*1,2,9]

[1]Department of Chemistry, National University of Singapore, 3 Science Drive, Singapore 117543, Singapore.

[2]Centre for Advanced 2D Materials, National University of Singapore, 6 Science Drive 2, Singapore 117546, Singapore.

[3]School of Chemical and Biomedical Engineering, Nanyang Technological University, 70 Nanyang Drive, Singapore 637457, Singapore.

[5]Australian Synchrotron Clayton, Victoria 3168, Australia.

[6]School of Chemistry, Physics and Mechanical Engineering, Queensland University of Technology, Brisbane, Queensland 4001, Australia.

[7]I10, Diamond Light Source Ltd, Diamond House, Harwell Science & Innovation Campus, Didcot, Oxfordshire, OX11 0DE, UK.

[8]NTU-Northwestern Institute for Nanomedicine, Nanyang Technological University, 50 Nanyang Avenue, Singapore 639798, Singapore.

[9]Hybrid Materials for Opto-Electronics Group, Department of Molecules and Materials, Faculty of Science and Technology, University of Twente, 7500 AE Enschede, The Netherlands

[†]These authors contributed equally

*E-mail: chmnca@nus.edu.sg, slim@ntu.edu.sg

Experimental details

S1. Materials

We purchased gold (Au) and silicon wafers (100, p-type, 500 ± 25 μm) with one side polished from Super conductor Materials, Inc. (USA) and University Wafers (USA), respectively. The 6-merhaptohexanoic acid, polydimethylsiloxane (PDMS), the gallium-indium eutectic (EGaIn) 75.5 % Ga and 24.5 % In by weight were purchased from Sigma. EDC was purchased from TCI chemicals. The solvents utilised were AR grade and purified by distillation before utilisation.

S2. E2-LFtn production and purification

Expression and purification of E2-LFtn was performed as described elsewhere with some modifications.[1] The production was carried out in E. *coli* BL21(DE3) cells (Stratagene, Santa Clara, CA). Protein was purified in 20 mM Tris, 5 mM (ethylenediaminetetraacetic acid) EDTA (pH 8.5) by anion exchange chromatography using Hi Prep QFF 16/10 column (GE Healthcare). The purified protein was then transferred to (4-(2-hydroxyethyl)-1-piperazineethanesulfonic acid) HEPES buffer (25 mM, pH = 8) by using 100 kDa Molecular Weight Cut-Off (MWCO) filters (Millipore, Billerica, MA) and stored at 4 °C until further use.

S3. Iron loading in E2-LFtn

Purified E2-LFtn (0.25 mg/ml in 25 mM HEPES, 50 mM NaCl, pH= 8) was loaded with iron by adding the required molar excess of ferrous sulphate hexahydrate in 0.1% HCl in steps of 500 atoms per cage every 15 minutes. Samples were incubated at room temperature (RT) for 1 hour followed by overnight storage at 4 °C. Unbound iron was removed by

desalting with Amicon centrifugal filters (100 kDa MWCO; Millipore, Billerica, MA). Iron quantification was performed using inductively coupled plasma atomic emission spectroscopy (ICP-OES) and protein quantification using Bradford assay. The iron content per cage of E2-LFtn was calculated by dividing the molar concentration of the iron obtained by ICP analysis by the molar concentration of E2LFtn obtained from Bradford assay. Figure S1A shows the dynamic light scattering spectra for apo-E2-LFtn and Fe-ion loaded E2-LFtn which are very similar from which we conclude that the globular geometry is retained after Fe-ion loading. Figure S2 shows the results of the Fe ion loading quantification which was found to be ±10% of the expected number.

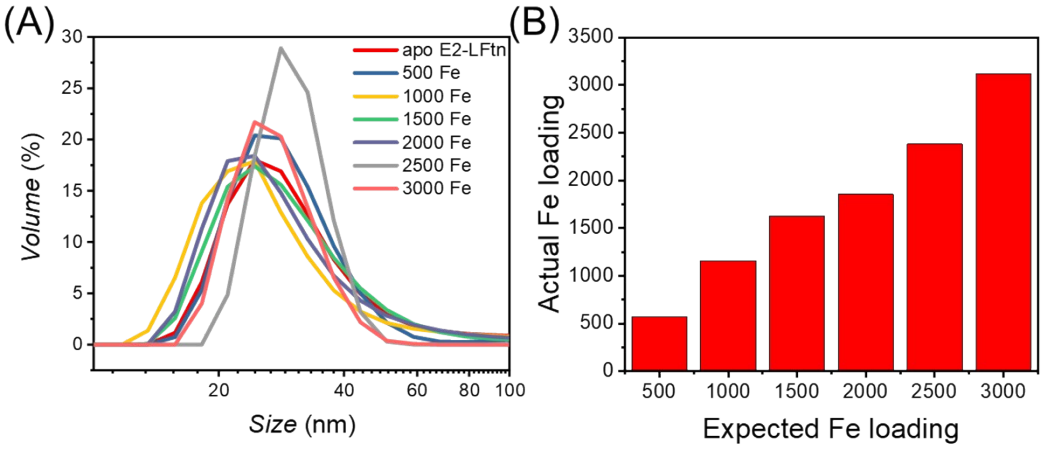

Figure S1: (A) Dynamic light scattering spectra of apo E2-LFtn and E2-LFtn samples and (B) Fe loading in the protein core vs. the expected Fe loading in the E2-LFtn samples obtained via inductively coupled plasma atomic emission spectroscopy.[1,2]

S4. Template stripped Au

We used a previously reported method[3] to prepare the ultra-smooth Au substrates (Figure 1). Briefly, we evaporated 150 nm of Au at a rate of 0.5 Å/s by using a thermal evaporator (ShenYang KeYi) at ~10^{-6} mbar. Glass slides were cleaned with piranha solution

(30% H_2O_2: concentrated H_2SO_4 = 1:3) for 15 min, then rinsed thoroughly with deionised water and finally dried under a dinitrogen stream. After that, we used a thermal adhesive (Epotek 353 ND) to glue the slides onto the Au surface followed by curing at 80°C in an oven for 2 hours.

S5. E2-LFtn monolayer on Au

The self-assembled monolayer of E2-LFtn on Au surface was prepared by a similar method as reported before for ferritin monolayers on Au surface, as illustrated in scheme 1.[2] First, the Au substrates were immersed in a 5 mL 6-mercaptohexanoic acid solution of 5 mM in EtOH overnight under an inert atmosphere. They were subsequently rinsed with EtOH and dried with flow of N_2 gas. Then, the substrates were activated in aq. 1-ethyl-3-(3-dimethylaminopropyl)carbodiimide (EDC, 5 mg/ 100 mL) solutions for 2 h, rinsed with deionised water and dried. Finally, the substrates were immersed in E2-LFtn solutions (overnight), rinsed with deionised water and dried prior to characterisation.

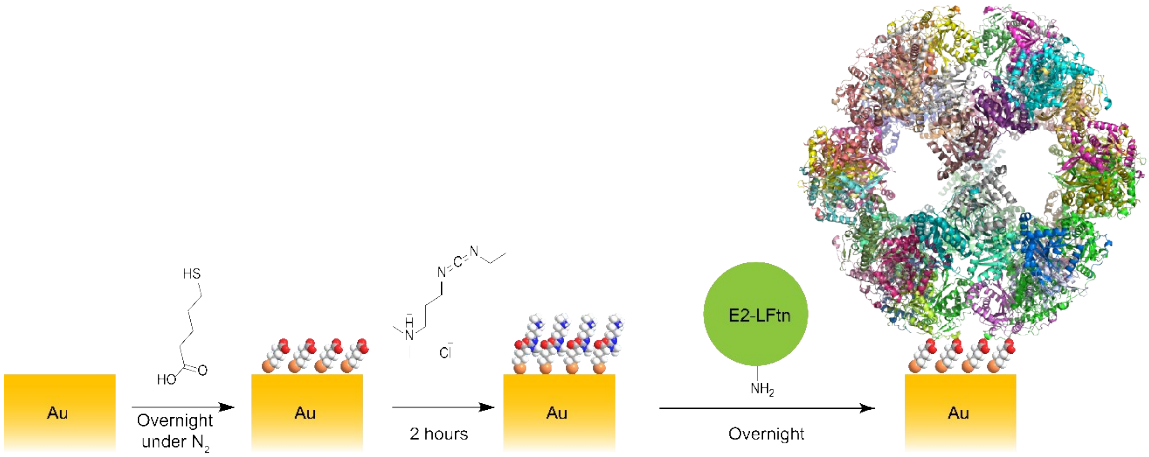

Scheme 1: Schematic illustration of the immobilisation of E2-Lftn onto Au electrodes via EDC activated 6-mercaptohexanoic acid linker.

S6. Atomic force microscopy (AFM)

The AFM images were obtained by Bruker dimension Fastscan AFM with tapping mode (FASTSCAN-A, resonant frequency: 1.4 MHz, force constant: 18 N/m). We used a Nanoscope Analysis (version 1.4) software to analyse the AFM images.

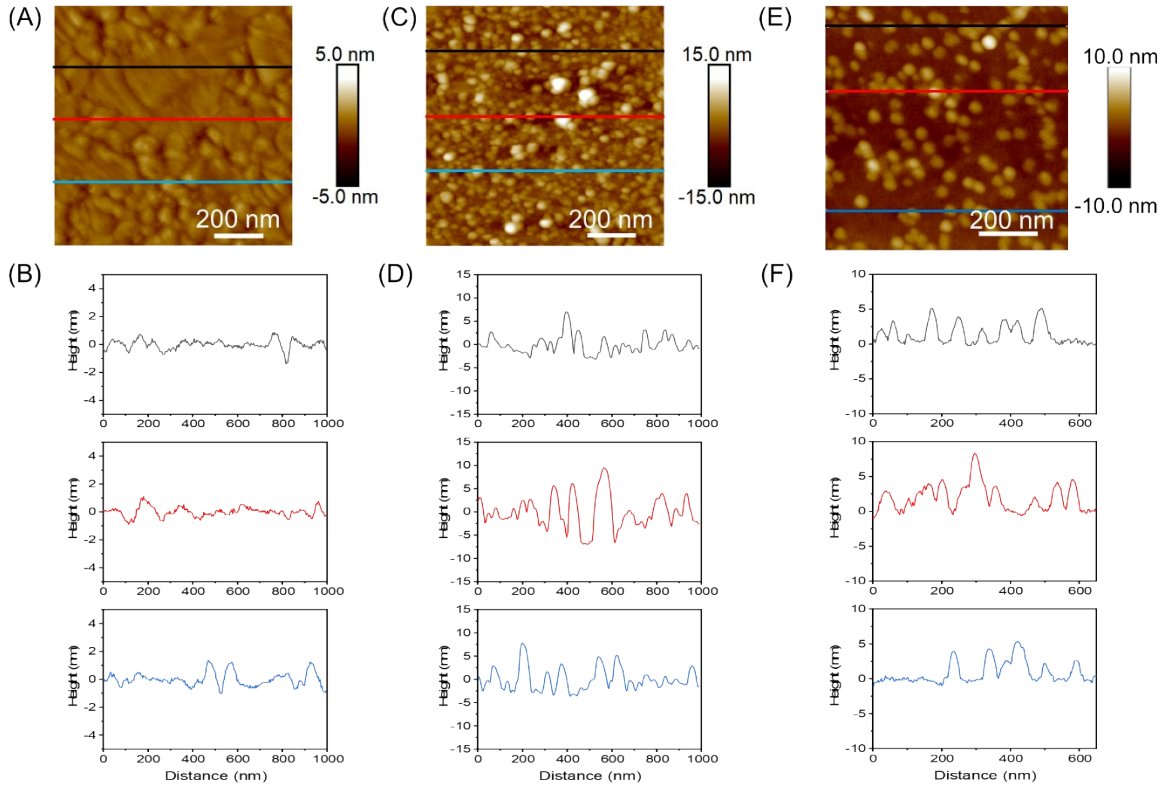

Figure S2: AFM images and the line scans for bare Au surfaces (A) and (B), respectively, and the same for 1000Fe E2-LFtn on Au (C) and (D), and a sub-monolayer of apo-E2-LFtn on Au (E) and (F).

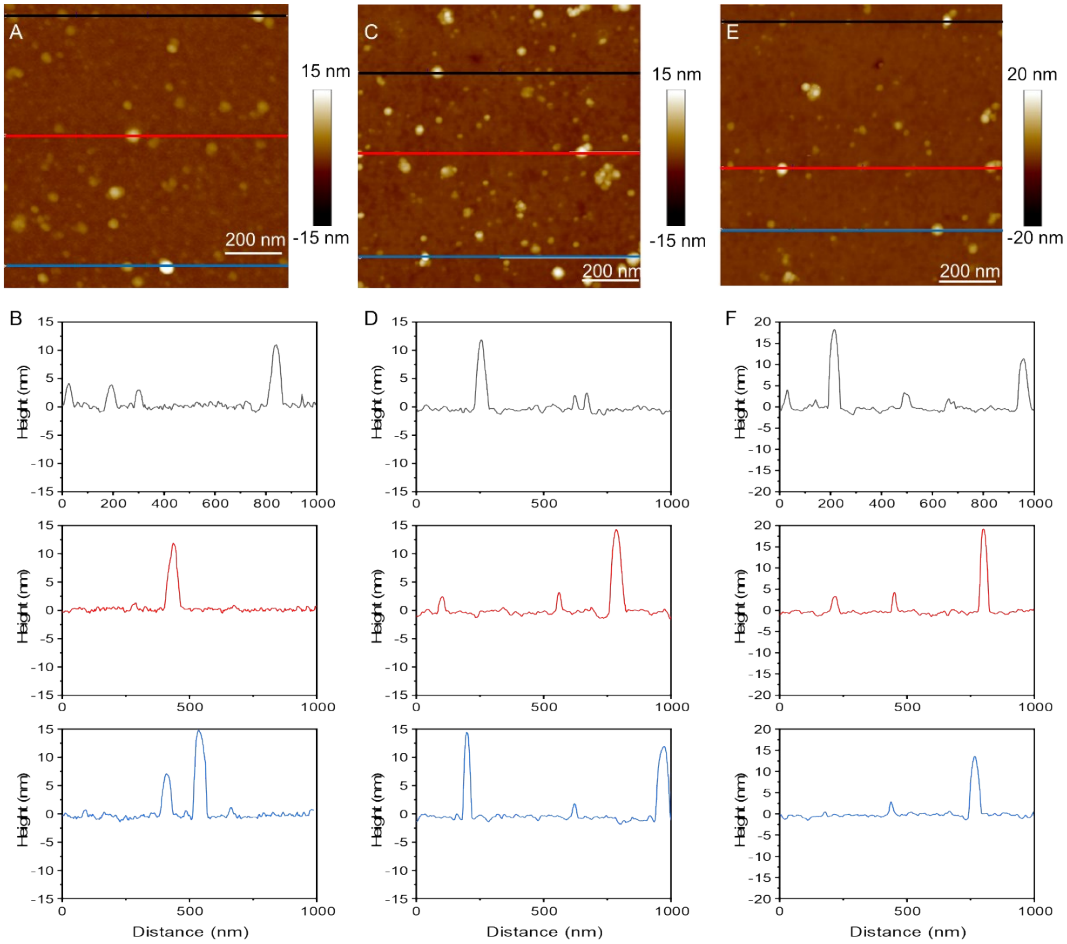

Figure S3: Additional examples of AFM images and the corresponding line scans of (A) and (B) 1000Fe LFtn, (C) and (D) 2000Fe E2-LFtn, and (E) and (F) 3000Fe E2-LFtn submonolayers that were used to estimate the $d_{\text{E2-LFtn}}$.

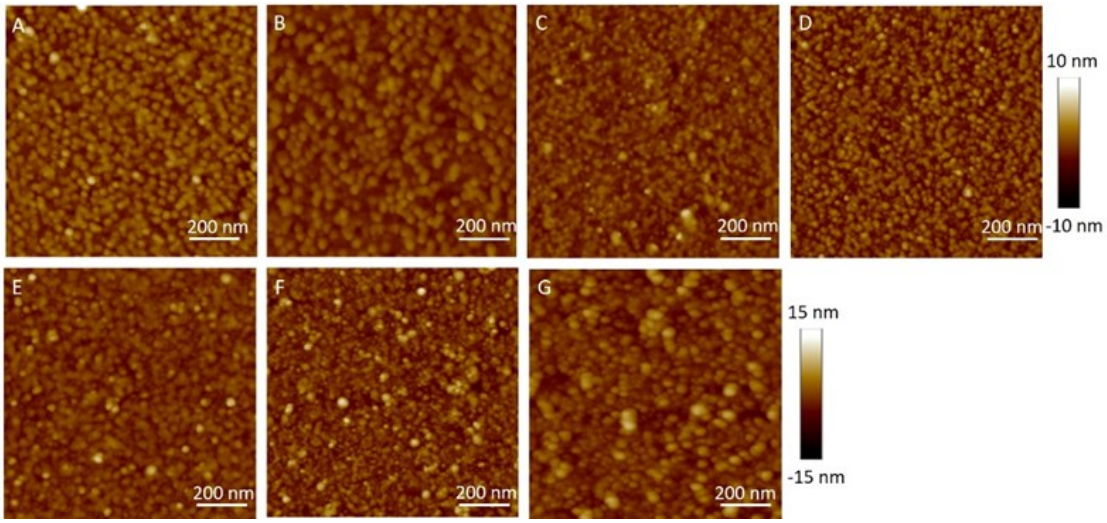

Figure S4: AFM images of monolayers of (A) apo-E2-LFtn, (B) 500Fe, (C) 1000Fe, (D) 1500Fe, (E) 2000Fe, (F) 2500Fe and (G) 3000Fe E2-LFtn.

S7. XAS

The Fe L-edge XAS measurements were performed at the soft X-ray beamline of Australian Synchrotron in TEY (total electron yield) mode following previously reported procedures.[4] The step size of 0.1 eV was used over the energy range of 700 – 730 eV. We used the Quick AS NEXAFS Tool (QANT)[5] to normalise the spectra to the incident photon flux. To extract a relative quantification of the oxidation state of iron in the E2-LFtn samples, we used a linear combination of simulated Fe^{II} and Fe^{III} spectra using the CTM4XAS software and followed a previously reported method to generate the spectra with parameters obtained from the crystallographic data of the specific iron ion components.[6] The crystal field splitting energy (10 Dq) was set at 1.6 for O_h sites and -0.6 for T_d sites, the d–d direct Coulomb parameters were set at 70% of the Hartree–Fock values, and the p–d direct and exchange values are at 80%, and the level broadening was set to 0.3 eV at the L_3 edge and 0.6 at the L_2 edge.[7] A linear combination of the simulated spectra of only three species, Fe^{2+} (O_h), Fe^{3+} (T_d), and Fe^{3+} (O_h), was used to model the raw data. The integrated intensity of each

component was used to estimate the R_I. The Fe^{II} and Fe^{III} ratios are presented for the modelling in Table S3. We kept the Fe^{II} relative concentration constant and only changed the Fe^{III} concentration to obtain good agreement between the modelled and the experimentally obtained spectra. As stated in the main text, we measured XAS under a high beam flux at the Diamond Line to ascertain the presence of iron oxide NPs in 2000Fe E2-LFtn at T = 300 K. We observe similar trends in the Diamond Line XAS dataset (Fig. S4 and Table S2) as compared to that obtained from the Australian Synchrotron (Fig. 3 and Table S1).

Table S1. Peak intensity ratio of 2000 Fe and 3000 Fe E2-LFtn at different temperature.

Sample	Fe^{II}	Fe^{III} [a]	R_I at 300 K	Fe^{II}	Fe^{III} [a]	R_I at 200 K	Fe^{II}	Fe^{III} [a]	R_I at 120 K
2000Fe	1.00	0.05	20.00	1.00	0.07	14.29	1.00	0.15	6.67
3000Fe	1.00	0.40	2.50	1.00	0.80	1.25	1.00	1.20	0.83

[a] The Fe^{3+} includes total contribution from Fe^{3+} T_d and Fe^{3+} O_h

[b] These experiments were carried out at the Diamond Light Source

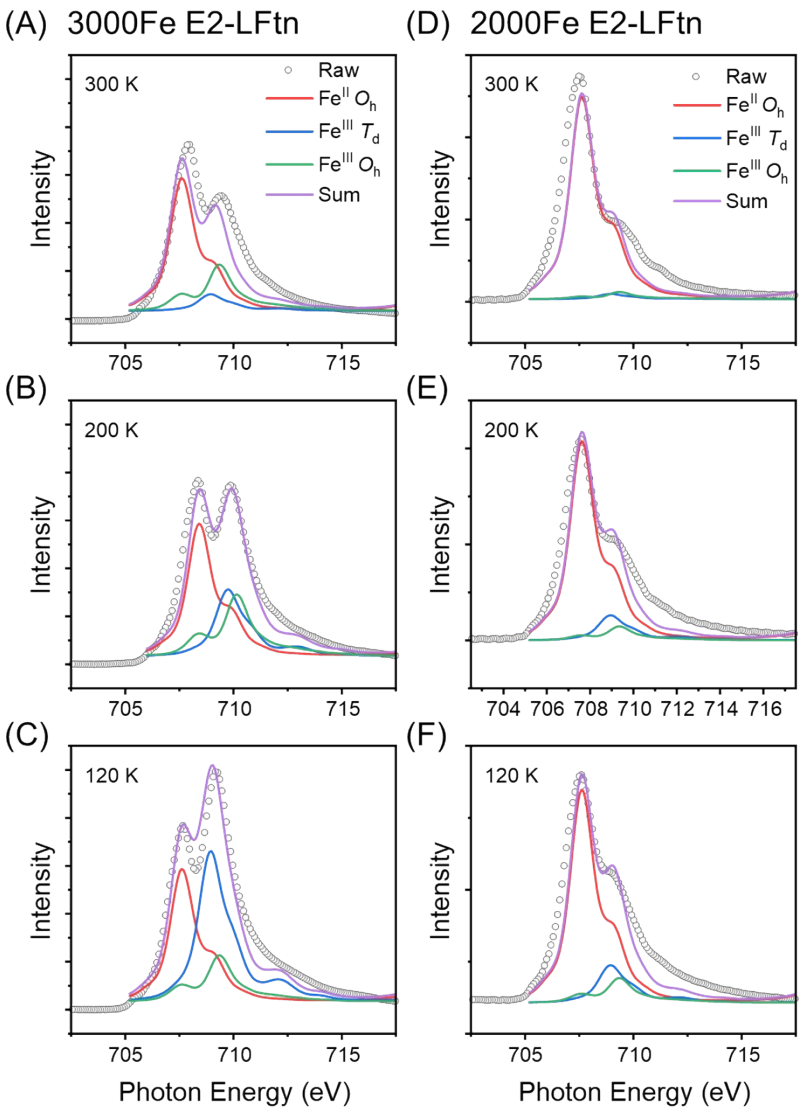

Figure S5: XAS spectra of 3000 Fe E2-LFtn at (A) 120 K, (B) 200 K and (C) 300 K, and 2000 Fe E2-E2-LFtn recorded at (D) 120 K, (E) 200 K and (F) 300 K) at the Fe L_3 edge.

Table S2. Peak intensity ratio of 2000 Fe and 3000 Fe E2-LFtn at different temperatures

Sample	Fe^{II}	Fe^{III} [a]	R_I at 300 K (initial)	Fe^{II}	Fe^{III} [a]	R_I at 120 K	Fe^{II}	Fe^{III} [a]	R_I at 300K (final)
2000Fe	-	-	-	1.00	0.50	2.00	1.00	0.20	5.00
3000Fe	1.00	0.80	1.25	1.00	2.00	0.50	1.00	1.00	1.00

[a] The Fe^{III} includes total contribution from Fe^{III} T_d and Fe^{III} O_h states
[b] These experiments were performed at the Australian Synchrotron

S8. EGaIn junction fabrication, *J*(*V*) data collection, and its analysis

We followed reported procedures to form the junctions.[8] A Keithley 6340 source meter was utilised to apply an external bias with LabView 2010 and to collect the *J*(*V*) data. The bias was changed from 0 V→ 1 V → 0 V → -1 V → 0 V. First, three scans were recorded for each junction to confirm the junction was stable. For stable junctions, we recorded 20 traces that all were used in our analysis. Junctions that shorted (compliance limit at 10^5 mA) or open circuits were not utilised in the data analysis. A summary of the *J*(*V*) data and junction yields are shown in Table S3. We followed the procedure for statistical analysis of the junction data as reported before.[9] The values of $\log_{10}|J|$ at each measured bias were plotted in a histogram, as shown in Figs. S3 and S4 for ±1.0 V and ±0.5 V, and a Gaussian was fitted to these histograms to obtain the log-average value of $|J|$, the log-standard deviation of J, $\sigma_{log,}$ and the 95% confidence bands. The $\log_{10}|J|$ and σ_{log} values are shown in Table S3.

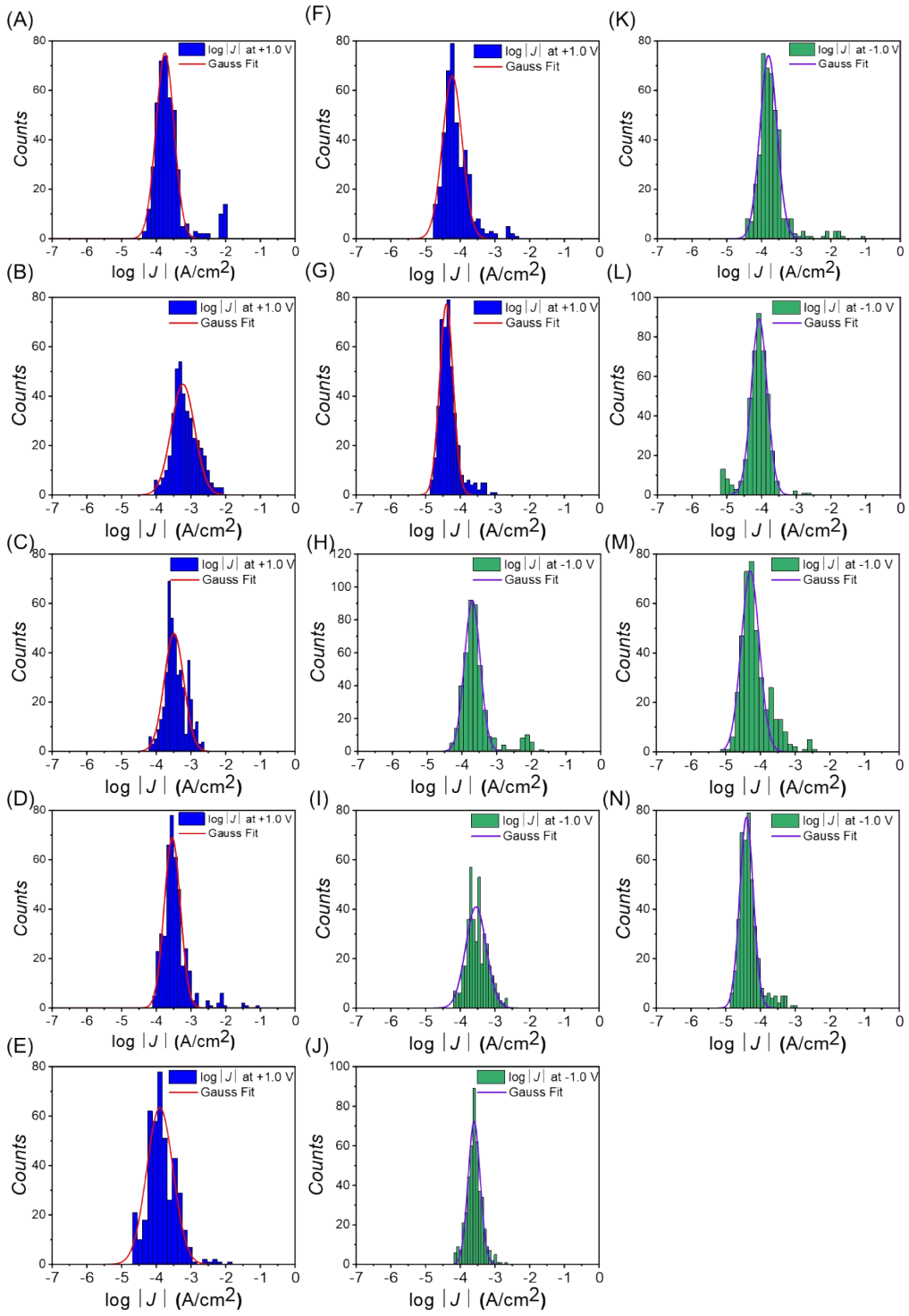

Figure S6: Histograms of log |*J*| obtained from Au-S-linker/E2-LFtn//GaO_x/EGaIn junctions measured at +1.0 V for A) apo E2-LFtn, B) 500 Fe, C)1000 Fe, D) 1500 Fe, E) 2000 Fe, F) 2500 Fe, G) 3000 Fe and at -1.0 V for H) apo E2-LFtn, I) 500 Fe, J)1000 Fe, K) 1500 Fe, L) 2000 Fe, M) and 2500 Fe, N) 3000 Fe. Solid lines are Gaussian fits.

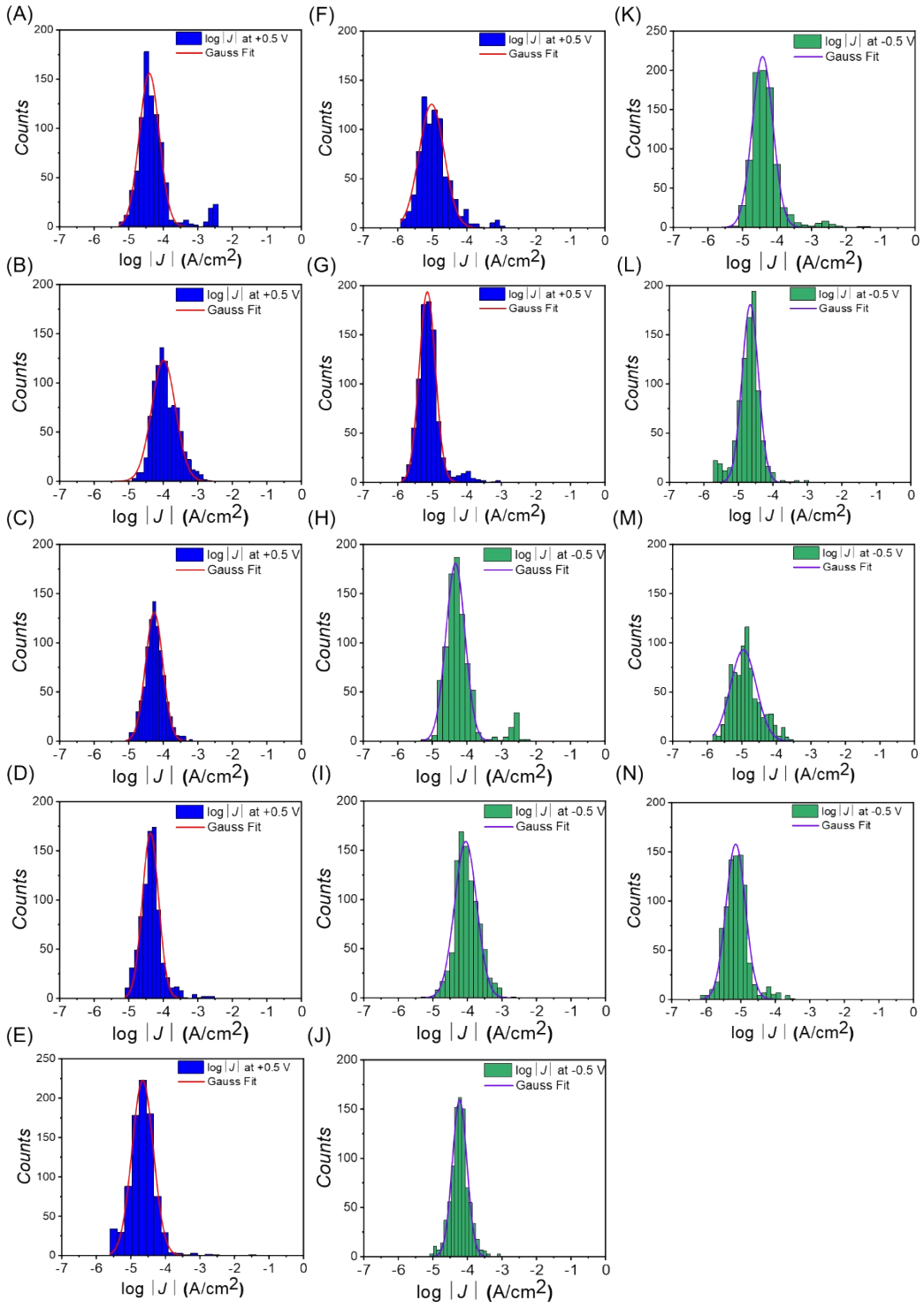

Figure S7: Histograms of log(|*J*|) obtained from Au-S-linker/E2-LFtn//GaO_x/EGaIn junctions measured at +0.5 V for A) apo-E2-LFtn, B) 500 Fe, C)1000 Fe, D) 1500 Fe, E) 2000 Fe, F) 2500 Fe, G) 3000 Fe and at -0.5 V for H) apo-E2-LFtn, I) 500 Fe, J)1000 Fe, K) 1500 Fe, L) 2000 Fe, M) 2500 Fe, and N) 3000 Fe. Solid lines are Gaussian fits.

Table S3. $d_{E2\text{-}LFtn}$ of E2-LFtn and apo-E2-LFtn and junction characteristics as a function of iron loading inside the E2 protein cage.

Molecule	Size (nm)	log |*J*| at -1.0 V (A/cm^2)	σ_{logG}	log |*J*| at +1.0 V (A/cm^2)	σ_{logG}	Junctions measured	Stable junctions	Stable traces	Yield (%)
Apo-E2-LFtn	6.9 ± 0.3	-3.69	0.23	-3.74	0.25	26	21	427	80.8
500 Fe	11.0 ± 0.3	-3.51	0.29	-3.1	0.40	33	26	475	74.3
1000 Fe	12.3 ± 0.5	-3.60	0.17	-3.50	0.26	25	20	439	80.0
1500 Fe	13.6 ± 0.3	-3.79	0.24	-3.53	0.23	26	22	422	84.6
2000 Fe	14.3 ± 0.4	-4.07	0.24	-3.90	0.37	26	20	425	76.9
2500 Fe	16.3 ± 0.4	-4.29	0.27	-4.24	0.28	22	20	397	90.9
3000 Fe	17.7 ± 0.4	-4.49	0.25	-4.40	0.20	22	21	422	95.5

S9. Micropore device fabrication

We followed a previously reported procedure to form micropore based junctions.[10] Briefly, Au strips (150 nm wide) along with contact pads were deposited on a Si wafer with its native SiO_2 layer by shadow mask deposition. Then the Si substrate was functionalised with 1H,1H,2H,2H-perfluorooctyltrichlorosilane to reduce the interaction of the thermal adhesive with the template to enable the template-stripping. Next, we applied the thermal glue (EPOTEK 353ND) and a glass support, cured the adhesive at 80 °C for 3 h and then we removed the glass/glue/Au composite from the template followed by deposition of 35 nm Al_2O_3 on the entire surface by atomic layer deposition at 90 C. Next, we prepared micropore with a diameter of 10 μm in the Al_2O_3 surface using standard e-beam lithography and two-step etching processes as reported before to expose the Au in the micropore. The SAMs were formed by the same method as described above. The top contact consisted of EGaIn stabilised in polydimethylsiloxane (PDMS) channels of 80 μm wide, 40 μm high, and 2 cm long perpendicularly aligned over the Au electrodes. The PDMS channels were aligned over the micropores under an optical microscope. The microchannels were filled with EGaIn with a syringe pump by applying a vacuum at a rate of 0.4–5.0 mm s^{-1} to complete the junctions.

S10. Temperature-dependent *J*(V) measurements

Measurements of *J*(V) as a function of temperature *T* (K) was carried out in a probe station (Lakeshore CRX-VF) at a pressure of 1.0×10^{-3} mbar as reported before.[2] The *J*(*V*,*T*) measurements were conducted in a temperature range of 340-200 K with steps of 10 K and 25 K in the 200-150 K temperature range. We restricted the temperature dependent *J*(*V*) measurements to 340 K, as the E2 protein undergoes denaturation at ~350 K.

S11. Switching measurements

Figure S7-8 presents the *J*(*V*,*T*) data of additional junctions with 3000Fe and 2000Fe E2-LFtn that were measured to demonstrate reproducibly. Figure S7A-B and D-E shows the cooling and heating cycles for 3000Fe E2-LFtn. As described in the main text, the junctions undergo conductance switching at $T = 220$ K in the cooling cycle and exhibit a nearly ~13-fold increase in current (Fig. S7C and E). The value of *J* restores to its initial value at 240 K in the heating cycle. Figure S8A and B show the cooling cycle from $T = 340 – 150$ K and the heating cycle $T = 150 – 300$ K for 2000Fe E2-LFtn. The junction switches at $T = 220$ K and this switching is irreversible. A ~40-fold increase in the current at $V = -0.8$ V is observed.

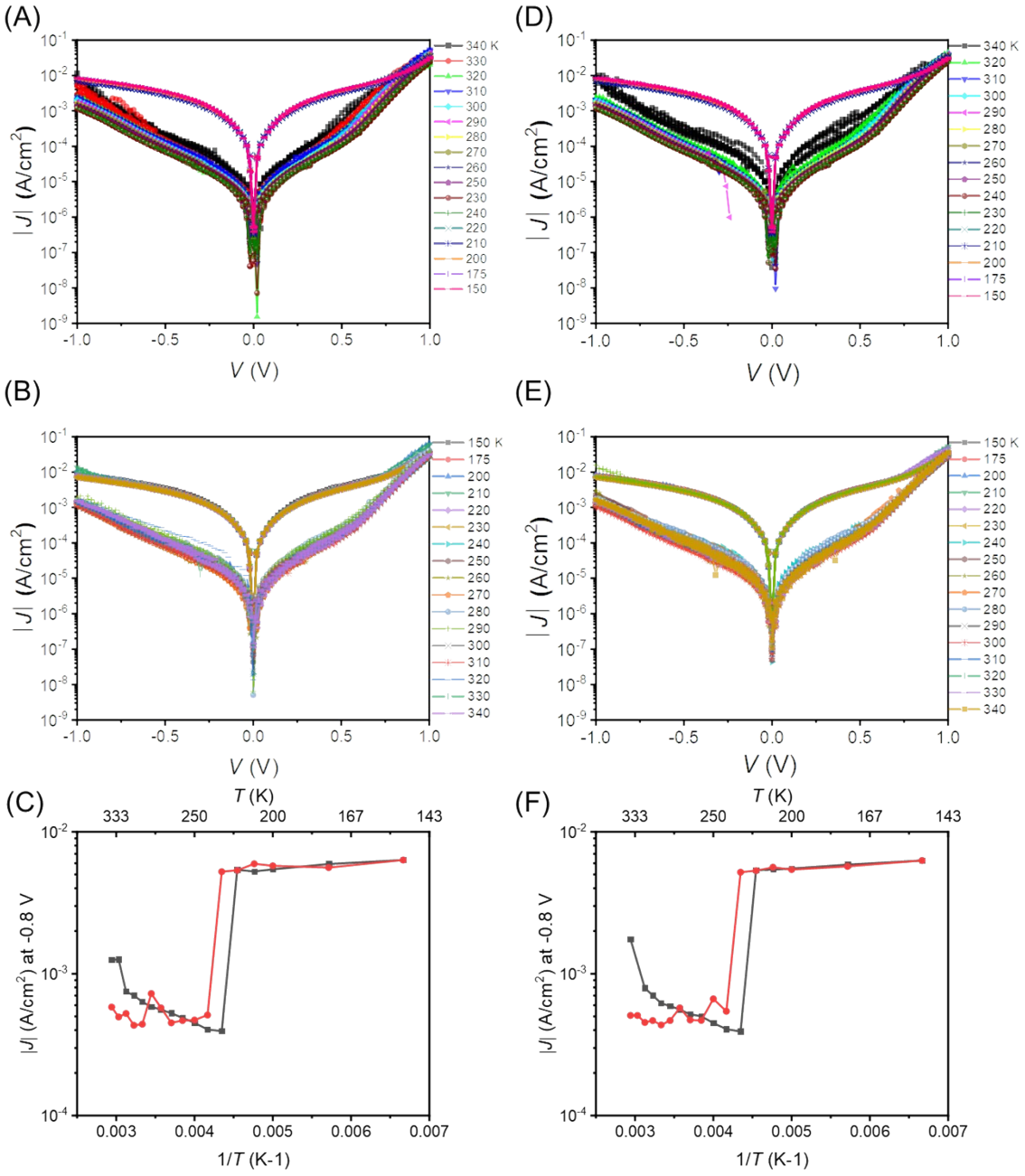

Figure S8: (A) and (B) show cooling and heating measurement for T = 340 – 150 K and (C) shows the value of J at V = -0.8 V for a 3000Fe E2-LFtn junction 2; (D-F) shows the same for junction 3.

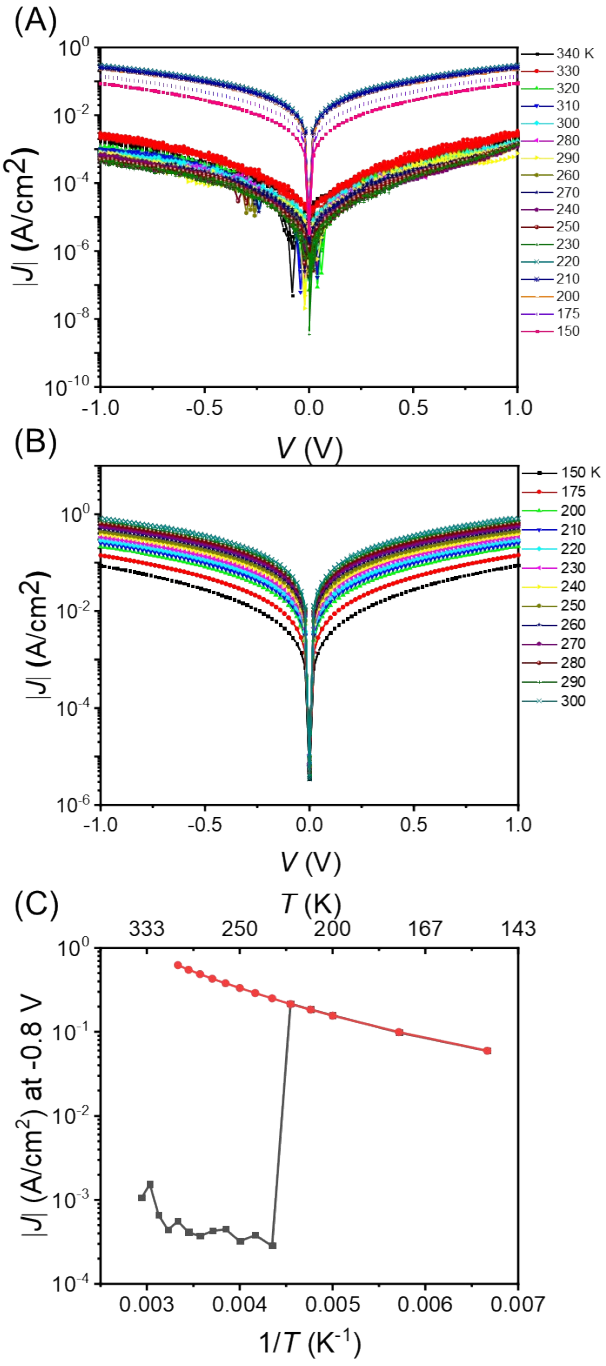

Figure S9: (A) and (B) show the cooling and heating measurement for T = 340 – 150 K and (C) shows the value of J at V = -0.8 V for junction 2.

References.

1 T. Peng, D. Paramelle, B. Sana, C. F. Lee and S. Lim, *Small*, 2014, **10**, 3131–3138.

2 K. S. Kumar, R. R. Pasula, S. Lim and C. A. Nijhuis, *Adv. Mater.*, 2016, **28**, 1824–1830.

3 K. Senthil Kumar, L. Jiang and C. A. Nijhuis, *RSC Adv.*, 2017, **7**, 14544–14551.

4 W. Du, Y. Han, H. Hu, H.-S. Chu, H. V. Annadata, T. Wang, N. Tomczak and C. A. Nijhuis, *Nano Lett.*, 2019, **19**, 4634–4640.

5 D. Cocco, E. Plönjes and M. Zangrando, *J. Synchrotron Radiat.*, 2016, **23**, 1–2.

6 E. Stavitski and F. M. F. de Groot, *Micron*, 2010, **41**, 687–694.

7 P. Kuiper, B. . Searle, L.-C. Duda, R. . Wolf and P. . van der Zaag, *J. Electron Spectros. Relat. Phenomena*, 1997, **86**, 107–113.

8 N. Nerngchamnong, L. Yuan, D.-C. Qi, J. Li, D. Thompson and C. A. Nijhuis, *Nat. Nanotechnol.*, 2013, **8**, 113–118.

9 H. J. Yoon, N. D. Shapiro, K. M. Park, M. M. Thuo, S. Soh and G. M. Whitesides, *Angew. Chemie - Int. Ed.*, 2012, **51**, 4658–4661.

10 S. K. Karuppannan, H. Hongting, C. Troadec, A. Vilan and C. A. Nijhuis, *Adv. Funct. Mater.*, 2019, **1904452**, 1904452.